Towards a better understanding of the epoxy-polymerization process using multi-objective evolutionary computation

Kalyanmoy Deb[a,*], Kishalay Mitra[b], Rinku Dewri[c], Saptarshi Majumdar[d]

[a] *Mechanical Engineering Department, Indian Institute of Technology Kanpur, Kanpur 208016, India*
[b] *Engineering and Industrial Services, Tata Consultancy Services, 54B Hadapsar Industrial Estate, Pune 411013, India*
[c] *Department of Mathematics, Indian Institute of Technology Kharagpur, Kharagpur 721302, India*
[d] *Tata Research Development and Design Centre, 54B Hadapsar Industrial Estate, Pune 411013, India*

Abstract

The epoxy-polymerization process can be better understood by investigating the underlying optimization problem involving a number of conflicting objectives and more than 20 decision parameters. A combination of minimization or maximization of objectives, such as the number average molecular weight, polydispersity index and reaction time, are considered in this paper. The first two objectives are related to the properties of a polymer, whereas the third objective is related to productivity of the polymerization process. The decision variables are addition quantities of various reactants, e.g. the amount of addition for bisphenol-A (a monomer), sodium hydroxide and epichlorohydrin at different time steps (modeled in a semi-batch operation), whereas the satisfaction of all species balance equations is treated as constraints. A multi-objective evolutionary algorithm (the elitist non-dominated sorting genetic algorithm or NSGA-II) is used to obtain a set of non-dominated solutions in a single simulation run. The results show a substantial improvement (with about 300% more productivity) over the benchmark condition (reported by performing a one-time addition of reactants in the beginning in a batch process). Importantly, this study brings out a salient aspect of using an evolutionary approach to multi-objective problem solving. The availability of multiple optimal trade-off solutions allows a process engineer to have salient information about the polymerization process. Changes in the distribution of various polymer species in the course of polymerization process as observed among various Pareto-optimal solutions are identified and explained for this purpose. Such information provide important information about optimal operating conditions corresponding to different trade-offs among objectives, which are otherwise difficult to obtain. The systematic approach of starting from the two-objective problems to capture the essential features of interesting optimal operating conditions to finally solving the three-objective problem associated with the epoxy-polymerization problem in discovering the optimal trade-off interactions should motivate further such studies on other chemical process optimization problems. Overall, this paper demonstrates how fundamental optimization principles can be used systematically and reliably to find optimum operating conditions for complex chemical process operations.

Keywords: Polymerization; Kinetics; Modeling; Optimization; Dynamic simulation; Multi-objective optimization; Pareto-optimal solutions; Genetic algorithms; Operating chart

1. Introduction

Epoxy-polymerization process, being quite complex in nature, can be posed as an optimization problem involving a number of conflicting objectives and time-varying decision variables. In modeling the polymerization process, several molecular parameters, such as the number or weight average molecular weights (M_n or M_w, respectively), the polydispersity index (PDI), concentration of different functional groups etc., can all be predicted accurately using various experimentally measured indices such as strength and stiffness of the final product. Moreover, the desired objectives in a polymerization process often exhibit conflicting relationships and

* Corresponding author. Tel.: +91-512-259-7205; fax: +91-512-259-7408.
E-mail addresses: deb@iitk.ac.in (K. Deb), kishalay.mitra@tcs.com (K. Mitra), rinku@webteam.iitkgp.ernet.in (R. Dewri), saptarshi.m@tcs.com (S. Majumdar).

therefore become an ideal problem to be treated truly as a multi-objective optimization problem. In this paper, multi-objective optimization of a semibatch epoxy-polymerization system, which is often used to manufacture high-strength composites, reinforced plastics, adhesives, protective coatings in appliances, etc., is performed to better understand the complex interaction of salient objectives involved in the epoxy-polymerization process.

Multi-objective optimization problems lead to a set of optimal solutions, known as *Pareto-optimal* solutions, as opposed to the single solution provided by any single-objective optimization task. Although only one solution must be chosen at the end of the optimization task and this often must be performed with the guidance of a decision-maker, it is a better practice to first find a set of Pareto-optimal solutions to have an idea of the extent of trade-offs possible among the underlying objectives before focusing on a particular solution (Deb, 2003). There are mainly two approaches to find a set of Pareto-optimal solutions: (i) single-objective preference-based methods, in which multiple objectives are scalarized into a single objective by means of certain preference information (Chankong and Haimes, 1983; Miettinen, 1999) and multiple applications of the approach are conducted to find a set of Pareto-optimal solutions and (ii) evolutionary multi-objective optimization (EMO) methods, in which multiple Pareto-optimal solutions are found simultaneously in a single simulation run (Deb, 2001). It is needless to write that the second approach may be preferred simply due to the time and effort saved in simultaneous computation of Pareto-optimal solutions.

Although the field of research and application on multi-objective optimization is not new, the use of EMO techniques in various engineering and business applications is a recent phenomenon.

A recent review by Bhaskar et al. (2000) reveals that several studies are carried out on multi-objective optimization of polymerization reactors. Tsoukas et al. (1982), Fan et al. (1984), Farber (1986, 1989), Butala et al. (1988), and Choi and Butala (1991) carried out multi-objective optimization of copolymerization reactors. These studies used Pontryagin minimum principle coupled with the ε-constraint method (Chankong and Haimes, 1983) to obtain a Pareto-optimal set of non-dominated solutions. Wajge and Gupta (1994) studied multi-objective optimization of the nylon-6 batch reactor and obtained different optimal temperature histories corresponding to different solutions on the Pareto-optimal set using the same technique. Sareen and Gupta (1995) extended that work, studied the nylon-6 semibatch reactor, and obtained different optimal pressure histories and optimal jacket fluid temperature corresponding to different solutions on the Pareto-optimal set. The solution technique used in these studies requires as many simulation runs as the desired number of distinct Pareto-optimal solutions, since each simulation run leads to a single Pareto-optimal solution. To alleviate this difficulty, a number of studies using an EMO approach are carried out on the multi-objective optimization of nylon-6 and polymethyl methacrylate (PMMA) reactors (Chakravarthy et al., 1997; Mitra et al., 1998; Garg and Gupta, 1999; Garg et al., 1999; Gupta and Gupta, 1999). These studies are mainly based on adapted version of the non-dominated sorting genetic algorithm (NSGA) developed by Srinivas and Deb (1995). In all these studies, constraints were handled using the standard penalty function method. It is well known in the optimization literature that the tuning of penalty parameters is a crucial issue in penalty-based-constraint handling methods. The NSGA procedure is modified by its developers to remedy this problem and to introduce a few other important features in the development of NSGA-II (Deb et al. (2002)). The use of a novel constraint-handling approach requiring no penalty parameter is a major improvement, which has made the NSGA-II quite efficient in solving constrained multi-objective optimization problems. We shall give a brief overview of the NSGA-II procedure in Section 3.

In the Taffy process (Kumar and Gupta, 1987), the most popular industrial process for preparing epoxy polymers, bisphenol-A (monomer) and epichlorohydrin, in excess, are reacted in presence of sodium hydroxide (NaOH) leading to the formation of polymer which is having glycidyl ether end group (building block) at both the ends. In the advancement process (McAdams and Gannon, 1986), the other route, pulverized sodium hydroxide is added in steps to the reaction mixture of bisphenol-A and epichlorohydrin dissolved in a solvent. It is well established that in all commonly used industrial processes of epoxy polymerization, alkali has a key role, which is usually added in semi-batch mode. Alkali controls oligomeric impurities in the advancement process (Kumar and Gupta, 1987; Ray, 1972). But the role of addition of other reactants (bisphenol-A and epichlorohydrin) is not well established. Experimental and theoretical studies are very few in open literatures for the epoxy-polymerization process. Studies on optimization of epoxy reactors are very rare according to the knowledge of the authors. Raha and Gupta (1998) used species balance and equation of moments approach to study the process. They gave special importance to build the entire modeling framework as well as the effect of kinetic parameters and reactant's effect over the performance of the reaction process. This work was extended elsewhere (Majumdar et al., 2004; Raha et al., 2004) with single and multi-objective optimization studies showing the effect of different addition amounts and patterns over the performance of the process. These past studies motivated us to launch this present detail study for a better understanding of the true nature of interactions among three-conflicting objectives associated with the epoxy-polymerization process.

In the remainder of the paper, we formulate the epoxy-polymerization process as a couple of two-objective optimization problems leading to a three-objective optimization problem. The formulation of associated constraints and the choice of decision variables are explained. Thereafter, a brief introduction to the NSGA-II procedure is given highlighting the constraint-handling strategy. The simulation results

of NSGA-II are then described and supported by comparing them with a number of single-objective preference-based optimized solutions. The interesting task of revealing important insights about the polymerization process is illustrated next by analyzing the obtained Pareto-optimal solutions. Finally, all the information gathered by the two and three-objective optimization tasks are combined together to understand the true trade-off among the three-conflicting objectives considered in this study, and important and useful conclusions are derived.

2. Formulation

In this section, we formulate the epoxy-polymerization problem as multi-objective optimization problems of various degrees of difficulty.

2.1. Model

The complete kinetic scheme for the above-mentioned polymerization system is given in appendix and can also be found elsewhere (Batzer and Zahir, 1977). Recently, Raha and Gupta (1998) and Majumdar et al. (2004) have validated the model with the available experimental data. Using the species balance approach, ODEs corresponding to the initial value problem (IVP) are derived for 10 molecular species and their moments. These equations are solved by an explicit numerical integration routine and kinetic parameters appearing in the equations are estimated with the help of a genetic algorithm (GA). Details on the modeling aspect, the solution procedure and the parameter estimation can be found in Majumdar et al. (2004). Here, we briefly describe the mathematical model.

The "state" of the reaction scheme can be well described by a set of 48 state variables ($\mathbf{x} = (x_1, x_2, \ldots, x_{48})^{\mathrm{T}}$), including all species balance and moment balance equations. Equations for these can be written using mass balance equations and by obtaining balance of moments of various orders. The state variable equations, in general, can be written in the form

$$\frac{\mathrm{d}x_i}{\mathrm{d}t} = f_i(\mathbf{x}, \mathbf{U}), \quad i = 1, 2, \ldots, 48, \tag{1}$$

where $\mathbf{x}$ and $\mathbf{U}$ are vectors of the state and decision variables (such as intermediate additions for different reactants at different times). The decision variable vector consists of three discrete histories, namely, discrete time history for NaOH addition (described here with $U_1(t_j)$), discrete time history for epichlorohydrin addition ($U_2(t_j)$) and discrete time history for bisphenol-A addition ($U_3(t_j)$), where t_j is the jth time instant at which the reactants are added.

The various molecular species including the monomer considered for the modeling exercise can be found elsewhere (Majumdar et al., 2004; Raha and Gupta, 1998). Mole balance equations for the end groups and lower oligomers in the batch reactor, the moment equations for various molecular species and the equations for number as well as average molecular weights are derived for this system. Given three discrete profiles of addition of reactants ($\mathbf{U}(t_j)$ at different discrete time steps t_j) and the initial conditions of all state variables ($\mathbf{x}$ at time zero), the complete mathematical model of the semibatch polymerization process can be solved by using an explicit integrator (a RK-type method is used here). This simulation procedure is then combined with the NSGA-II optimization procedure for performing a multi-objective optimization.

2.2. Defining the optimization problems

Three different multi-objective optimization problems are studied here. The first problem (Problem 1) is related to the quality of polymer produced, whereas the second problem (Problem 2) addresses the productivity issue also. The objective for Problem 1, $\mathbf{I}_1$, is a vector and consists of two objectives: The first (I_{11}) is the maximization of M_n and the second (I_{12}) is minimization of PDI. Thus, the simultaneous attainment of the two objectives has to be obtained with satisfying the mass and moment balance equations. A scheme of the reactions is shown in appendix. All 48 equations can be found elsewhere (Raha and Gupta, 1998; Majumdar et al., 2004). Simultaneous attainment of these two objectives is going to produce high quality polymers with different trade-offs between M_n and PDI values

$$\textbf{Problem 1}. \begin{cases} \text{Maximize} & I_{11} = M_n \\ \text{Minimize} & I_{12} = \text{PDI}, \\ \text{subject to} & \text{satisfying mass and moment balance equations}, \\ & u_i^{\min} \leqslant u_i \leqslant u_i^{\max}, \\ & i = 1, 2, \ldots, 21. \end{cases} \tag{2}$$

One computer simulation runs from zero (initial condition, $t = 0$) to $t = t_{\text{sim}}$ (7 h used here). Each of the three profiles ($U_1(t_j)$, $U_2(t_j)$, $U_3(t_j)$) are, therefore, discretized into seven equally spaced points (one for each time instant t_j), thereby making a total of $n = 21$ discrete values: u_1, u_2, …, u_{21}). This means that the decision variables u_1 to u_7 represent $U_1(t_j)$ (amount of addition of NaOH), u_8 to u_{14} represent $U_2(t_j)$ (amount of addition of EP) and u_{15} to u_{21} represent $U_3(t_j)$ (amount of addition of AA_0) at seven different times ($t_j = 0, 1, 2, 3, 4, 5, 6$ h). Each of these variables is forced to lie between a lower bound ($u_i^{\min}$) and an upper ($u_i^{\max}$) bound. No restriction on the M_n and PDI values are used, as the satisfaction of variable bounds will ensure limiting values on M_n and PDI.

The objective for Problem 2, $\mathbf{I}_2$, is a vector of two objective functions: The first (I_{21}) is the maximization of M_n and the second (I_{22}) is minimization of the overall reaction time, t_{sim}. Simultaneous attainment of these two objectives has to be obtained with satisfying the mass and moment balance equations. As the resultant product is supposed to obey the chemical principles due to the satisfaction of constraints, the

attainment of the second objective is going to ensure the optimal productivity (by reducing the reaction time). In short, this formulation improves productivity

$$\textbf{Problem 2}.\ \begin{cases} \text{Maximize} & I_{21} = M_n \\ \text{Minimize} & I_{22} = t_{\text{sim}}, \\ \text{subject to} & \text{satisfying mass and moment} \\ & \quad \text{balance equations}, \\ & u_i^{\min} \leqslant u_i \leqslant u_i^{\max}, \\ & \quad i = 1, 2, \ldots, 21, \\ & t_{\text{sim}}^{\min} \leqslant t_{\text{sim}} \leqslant t_{\text{sim}}^{\max}. \end{cases} \quad (3)$$

The reaction time t_{sim} is also a decision variable in this problem, thereby making the total number of variables to a maximum of $n = 22$. It is understood here that depending on the value of the reaction time variable, t_{sim}, the simulation time of the reaction scheme is going to be determined.

The objective for Problem 3, $\mathbf{I}_3$, is a vector of three objective functions: The first (I_{31}) is the maximization of M_n, the second (I_{32}) is minimization of t_{sim}, and the third (I_{33}) is the minimization of PDI. Simultaneous attainment of these three objectives has to be obtained with satisfying the mass and moment balance equations. On the one hand, the product quality is going to be assured by the first and third objectives and the constraints assigned on them, on the other hand, the attainment of second objective ensures productivity. In this problem, the reaction time t_{sim} is also a decision variable. This problem also has $N_{\text{Digit}} = 22$ decision variables

$$\textbf{Problem 3}.\ \begin{cases} \text{Maximize} & I_{31} = M_n \\ \text{Minimize} & I_{32} = t_{\text{sim}}, \\ \text{Minimize} & I_{33} = \text{PDI}, \\ \text{subject to} & \text{satisfying mass and moment} \\ & \quad \text{balance equations}, \\ & u_i^{\min} \leqslant u_i \leqslant u_i^{\max}, \\ & \quad i = 1, 2, \ldots, 21, \\ & t_{\text{sim}}^{\min} \leqslant t_{\text{sim}} \leqslant t_{\text{sim}}^{\max}. \end{cases} \quad (4)$$

3. Elitist non-dominated sorting GA (NSGA-II)

Contrary to the classical approaches, evolutionary multi-objective optimization (EMO) procedures aim at finding a finite, representative set of Pareto-optimal solutions in a problem. Fig. 1 illustrates this aspect on a hypothetical three-objective minimization problem. The task of an EMO procedure is to *identify* the Pareto-optimal front (shown separately as a surface) out of the entire feasible search space. This is, by no means, an easy task. Various optimization concepts must have to be used to clearly identify the true Pareto-optimal front. Starting from Section 4, we shall demonstrate how different optimization concepts can be used to unveil the Pareto-optimal front for the epoxy-polymerization problem and finally in Section 4.3 present the resulting front.

Although one optimal solution would be chosen at the end of the optimization task, a knowledge of the range of Pareto-optimal solutions is helpful in (i) choosing a particular

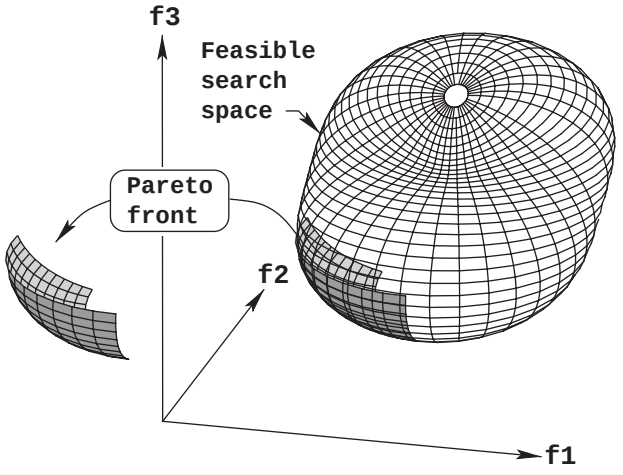

Fig. 1. A three-objective feasible region and the corresponding Pareto-optimal front.

optimal solution and (ii) getting useful insights about trade-off among objectives of the problem (Deb, 2003). Thus, the task of an EMO is to (i) converge to the true Pareto-optimal front and (ii) maintain a good distribution of solutions on the entire front. There exist a number of EMO techniques for this purpose (Deb, 2001). The elitist non-dominated sorting GA or NSGA-II procedure (Deb et al., 2002) for finding a well-distributed and well-converged set of multiple Pareto-optimal solutions in a multi-objective optimization problem is described here.

Like in a genetic algorithm (GA), NSGA-II starts with a population of N_{pop} random solutions. In the Nth iteration of NSGA-II, the offspring population Q_N is first created by using the parent population P_N and the usual genetic operators—reproduction, recombination, and mutation (Goldberg, 1989). Thereafter, both populations are combined together to form R_N of size $2N_{\text{pop}}$. Then, a non-dominated sorting procedure (Deb, 2001) is applied to classify the entire population R_N into a number of hierarchical non-dominated fronts. Fig. 2 shows a schematic of one iteration of NSGA-II.

Once the non-dominated sorting of the set R_N is over, the new population is filled with solutions of different non-dominated fronts, one at a time. The filling starts with the best non-dominated front and continues with solutions of the second non-dominated front, followed by the third non-dominated front, and so on. Since the overall population size of R_N is $2N_{\text{pop}}$, not all fronts may be accommodated in N slots available in the new population. All fronts which could not be accommodated are simply deleted. When the last allowed front is being considered, there may exist more solutions in the last front than the remaining slots in the new population. This scenario is illustrated in Fig. 2. Instead of arbitrarily discarding some members from the last front, the solutions which will make the *diversity* of the selected solutions the highest are chosen. In this step, the crowding–sorting of the solutions of front i (the last front

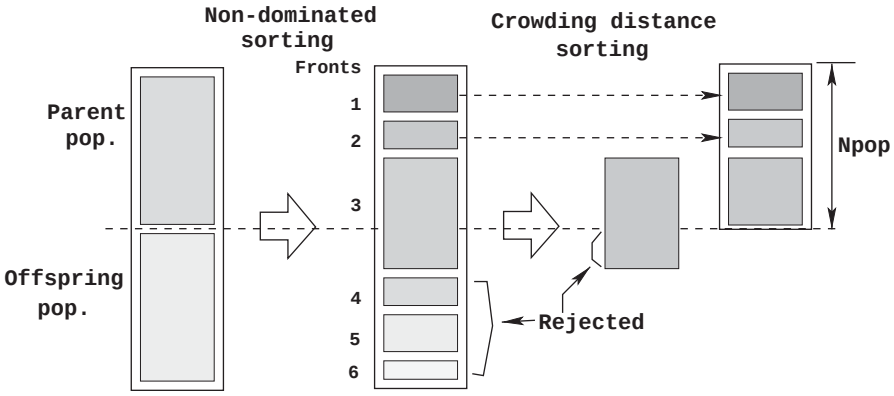

Fig. 2. Schematic of the NSGA-II procedure.

which could not be accommodated fully) is performed by using a *crowding distance metric* and the adequate number of solutions are picked from the top of the list. The crowding distance of a solution in a non-dominated front is a measure of crowding by other members of the front, In the NSGA-II implementation, a simple measure totalling the objective-wise distances between neighboring solutions is used. For details, readers are encouraged to refer to the original study (Deb et al., 2002). This study also showed that for N population members solving a M-objective problem, the computational complexity of one iteration of NSGA-II is $O(MN^2)$.

3.1. NSGA-II for the epoxy-polymerization problem

Each solution is represented as a real-valued vector of 21 (or 22 for Problems 2 and 3 with an additional variable t_{sim}) values indicating the addition of NaOH, EP, and AA_0. Thus, a solution with known values of these quantities can be evaluated by following the simulation procedure described earlier. The evaluation will produce two (or three for Problem 3) objective values. NSGA-II allows both minimization and maximization of different objectives by using the domination concept (Deb, 2001). Thus, the objectives are used straightway (without any transformation) as they are described in Eqs. (2)–(4). For the real-coded NSGA-II, we use the simulated binary crossover (SBX) and the polynomial mutation operators (Deb and Agrawal, 1995). For the binary-coded NSGA-II (mainly used here to gain confidence about the reported non-dominated solutions), we use a single-point crossover and a bitwise mutation operator (Goldberg, 1989). It is interesting to note that since solutions are always created within the specified lower and the upper bounds, the variable bounds will never be violated by both NSGA-IIs. Since the constraints are taken care of by solving the differential equations numerically, no explicit constraint handling strategy is used here.

When a pre-specified maximum iteration count ($N = N_{\max}$) is reached, NSGA-II is terminated and the non-dominated solutions of the final population are declared as the obtained Pareto-optimal solutions. In Problems 1 and 2, $N_{\max} = 200$ and a population size of $N_{\text{pop}} = 250$ are used. Since Problem 3 deals with a three-dimensional Pareto-optimal front, we have chosen a larger population size and run NSGA-II for more iterations: $N_{\text{pop}} = 1000$ and $N_{\max} = 500$. The crossover and mutation probabilities of $p_c = 0.9$ and $p_m = 0.1$ are used for the real-coded NSGA-II and of $p_c = 0.9$ and $p_m = 0.001$ for the binary-coded NSGA-II. For the SBX operator mentioned above the distribution index of 0.01 and for the polynomial mutation operator the distribution index of 0.01 are used. Each optimization procedure is run at least five times from different initial populations to build a confidence on the obtained optimized solutions.

4. Results and discussions

As mentioned earlier, the availability of experimental data for the epoxy-polymerization processes is really scarce. As far as authors' information is concerned, very little or no experimental or plant data is available for PDI and number averaged molecular weight (M_n) for the epoxy-polymerization system. This makes the entire modeling analysis extremely difficult, as validation of the modeling exercise cannot be done in terms of M_n and PDI. Raha and Gupta (1998) addressed this issue in an indirect way. They validated their moment-based model with the data of Batzer and Zahir (1977) for the monomer concentration profile. This is quite reasonable as after some hours of polymerization reactions, if the monomer concentration profile can be matched closely with the experimental data, that itself proves the validity of the proposed mechanism as well as the entire modeling exercise. In the present work the same approach is followed. Kinetic parameters are estimated from a parameter optimization exercise using a simple GA which is used to minimize the error between the simulated values and experimental data on certain monomer concentrations. Fig. 3 shows the match between the simulated results and experimental data of a primary

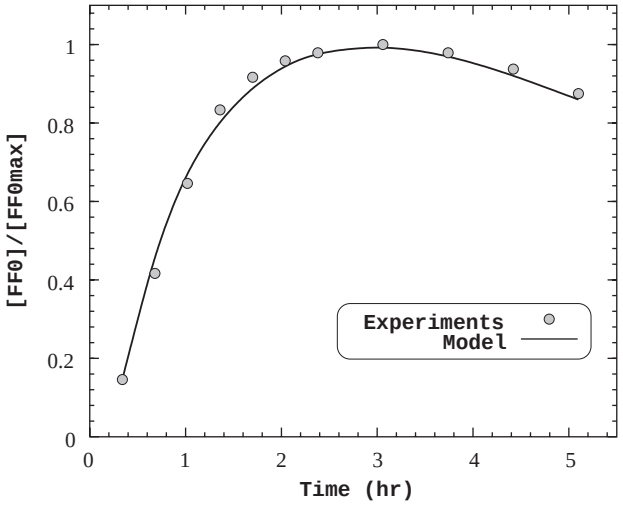

Fig. 3. Comparison of experimental data and the mathematical model in which kinetic parameters are obtained using a GA.

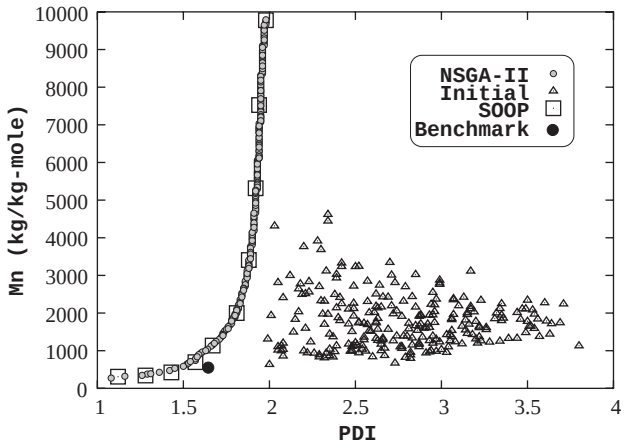

Fig. 4. Obtained NSGA-II solutions for the M_n and PDI optimization are compared with single-objective optimization (SOOP) solutions. Initial solutions of NSGA-II and the benchmark solution are also shown.

oligomer (FF_0). These parameters are used in the models of this paper to simulate various scenarios. Batzer and Zahir (1977) used 0.4 kmol/m^3 for NaOH, 1.280 kmol/m^3 for epichlorohydrin (EP), and 0.4 kmol/m^3 for bisphenol-A (AA_0) as initial concentrations for the three reactants. Based on this, following variable bounds are set here to allow the optimizer (NSGA-II) a substantial search space to look for the optimized solutions:

(1) The addition of NaOH varies between 0.2 and 1.0 kmol/m^3 at $t=0$ h and between zero and 1.0 kmol/m^3 for $t > 0$ h.
(2) The addition of EP varies between 0.2 and 2.0 kmol/m^3 at $t = 0$ h and between zero and 2.0 kmol/m^3 for $t > 0$ h.
(3) The addition of AA_0 varies between 0.2 and 1.0 kmol/m^3 for $t = 0$ h and between zero and 1.0 kmol/m^3 for $t > 0$ h.

4.1. Discussion on Problem 1

A simulation result corresponding to the initial condition of Batzer and Zahir (1977) (with $M_n = 633.2$ kg/kg mol and PDI = 1.61) is considered as the benchmark performance data with which our optimized solutions will be compared later. After the multi-objective optimization with NSGA-II, Pareto-optimal solutions are generated for the Problem 1 and are marked as "NSGA-II" solutions in Fig. 4. The solutions termed as "Initial" denote the objective vectors with which the NSGA-II search process is started (created by using random values of 21 decision variables within their respective bounds). The upper and lower bounds of the decision variables are used as stated earlier. The figure indicates that the random solutions (within the chosen variable bounds) are far from being close to the true Pareto-optimal front, particularly producing solutions with large M_n values and very small PDI values. Although a maximum of 200 iterations are scheduled, the real-coded NSGA-II took only 34 iterations to get the distribution shown in Fig. 4. The non-dominated front dictated by these solutions was not found to change thereafter. The figure clearly shows that a wide range of distribution in both M_n and in PDI values are obtained. The trade-off obtained between the two objectives is also clear from the figure. For the chosen variable bounds, this is the maximum trade-off possible between M_n and PDI values. The following observations can be made from the obtained results:

(1) The resulting M_n-PDI trade-off is *non-convex*, a phenomenon which is rare in real-world multi-objective optimization problems. Recall that here M_n is maximized and PDI is minimized.
(2) The NSGA-II progresses quite well from the initial population (which consists of solutions having small values of M_n and large values of PDI) to reach the final front having a wide range of M_n and PDI values.
(3) Investigating the solutions of Fig. 4 further, it can be inferred that compared to the benchmark solution (marked as 'Benchmark' in the figure) there exist better solutions in the system which can produce larger M_n (ranging from 645 to 966 kg/kg mol) and less PDI (ranging from 1.52 to 1.61, respectively) value, leading to polymers with better properties as compared to benchmark solution. In fact, the figure also clearly indicates that the benchmark solution is *dominated* by some NSGA-II solutions. If more than 1.61 PDI value is accepted in an application, M_n values much larger than the benchmark value can be achieved and once the PDI value increases beyond 1.8 or so, the corresponding M_n value is observed to increase at a fast rate.

4.1.1. Comparing with single-objective optimization results

In order to verify whether the obtained NSGA-II solutions can actually be close to the true Pareto-optimal front of this problem, we use a single-objective preference-based method next. Since, the above observation indicates that the Pareto-optimal front is non-convex, the commonly used weighted-sum approach (Chankong and Haimes, 1983; Miettinen, 1999) may not be the right approach for this problem, as the weighted-sum approach is known to fail in finding the Pareto-optimal solutions in the non-convex region (Deb, 2001). Thus, we use the ε-constraint method here (Miettinen, 1999). In this case, we convert the second objective (minimization of PDI) into an additional constraint as PDI$\leqslant$PDI$_\varepsilon$ and maximize only the first objective. Other constraints and variable bounds, as given in Problem 1, are kept the same. To obtain different Pareto-optimal solutions, we simply choose a different value for PDI$_\varepsilon$ and optimize the resulting single-objective optimization problem using a single-objective GA. The constraints are handled using a penalty parameter less procedure (Deb, 2000). The GA parameters, such as the population size, operator parameters, etc., are kept the same as those used in the above NSGA-II study. This approach must be applied as many times as the desired distinct Pareto-optimal solutions, since each single-objective optimization solution leads to only one solution on the Pareto-optimal front. Fig. 4 marks these solutions as 'SOOP' solutions obtained by 10-independent GA runs, each performed with a different PDI$_\varepsilon$ value. Since these solutions are found to lie on or near the Pareto-optimal front obtained by the NSGA-II, it can be stated that the Pareto-optimal front found by NSGA-II is probably the true Pareto-optimal front.

4.1.2. Comparing with binary-coded NSGA-II

Next, all 21 decision variables are coded in binary strings of seven bits each and the same NSGA-II is used, except that the real-coded crossover and mutation operators are replaced by single-point and bit-wise mutation operators. The comparative performance between real-coded and binary-coded NSGA-II is presented in Fig. 5, where it is observed that the real-coded NSGA-II performs slightly better than the binary-coded NSGA-II for higher values of M_n. Thus, the agreement of the results obtained from three procedures give us enough confidence on the optimality of the obtained solutions and more importantly on the performance of the real-coded NSGA-II on the two-objective epoxy-polymerization problem. Such a reliable and systematic procedure is rarely performed in other chemical process optimization studies. Here, we advocate following the above practice, particularly because in such problems the knowledge of *true* Pareto-optimal solutions is not known and investigators must try to use all available optimization tools to gain confidence about the optimality of the obtained solutions. We now discuss an interesting and important aspect of the obtained solutions advocated in this paper.

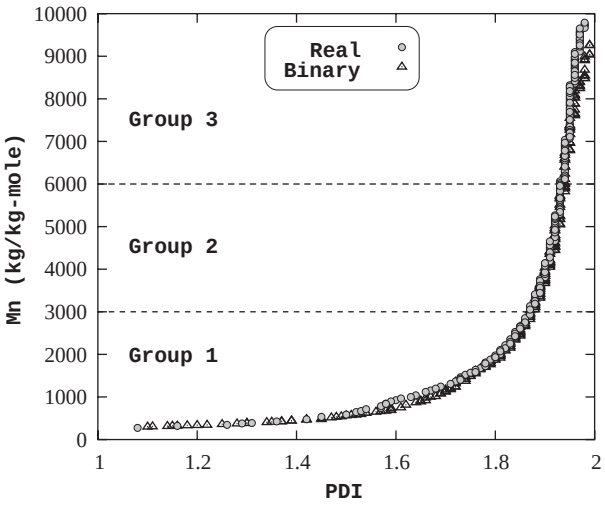

Fig. 5. Real-coded and binary-coded NSGA-II solutions for the M_n and PDI optimization.

4.1.3. Searching for salient properties of pareto-optimal solutions

Each of the solutions on Pareto-optimal front carries information about 21 decision variables. The Fritz–John necessary conditions for Pareto-optimal solutions (Deb, 2001; Miettinen, 1999) indicate that there exist a number of mathematical conditions which every Pareto-optimal solution must satisfy. This leads us to believe that the obtained solutions, if close to the Pareto-optimal solutions, will share some common properties among them and, of course, will have some differences in order to have trade-offs among them. If such properties exist, they would be worth searching for in a real-world application problem, as a knowledge of them will provide important and useful information about the optimal trade-off among objectives (Deb, 2003).

An investigation is performed next to identify whether the obtained M_n-PDI solutions bear some kind of similarity in terms of the associated decision variables. Interesting trends are discovered and shown in Fig. 6. Addition rates of all three ingredients for all obtained solutions are shown in the figure. Though the decision variables are discrete amount of addition of reactants at various time steps, they are joined with straight lines to show the trends. A casual look at the plots will reveal some interesting patterns followed in all obtained solutions. Although, the additions at every hour could have been anywhere on the vertical axis at each time step, all obtained solutions seem to follow some patterns. These patterns reveal important insights about the optimal working characteristics of the epoxy-polymerization problem, some of which we have deciphered and are discussed in the following:

(1) The general trend captured in NaOH addition is to start from the lower bound, reduce or increase the amount of addition at the first hour, increase close to the up-

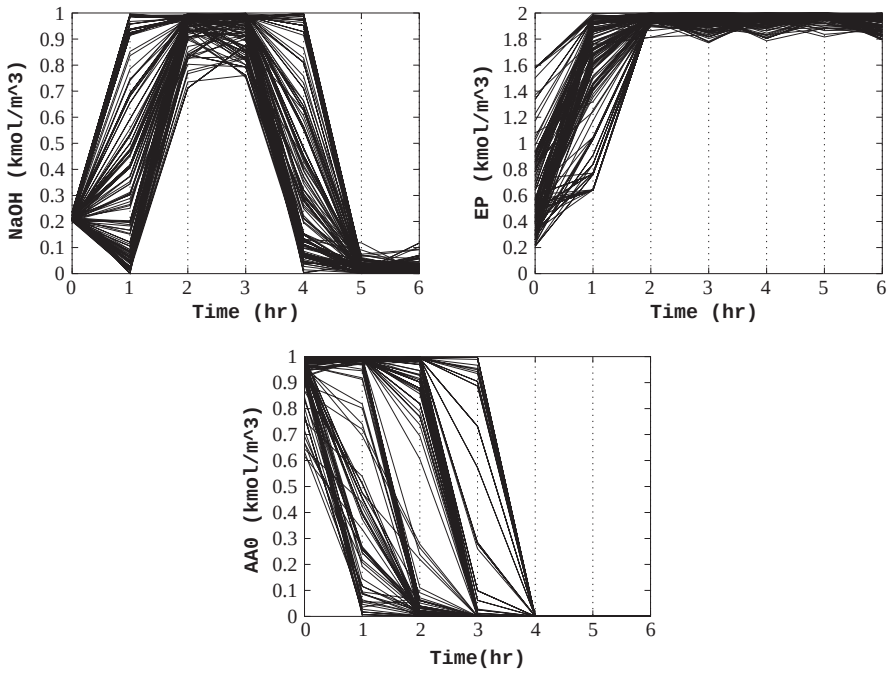

Fig. 6. Time-variant addition of NaOH (top-left), EP (top-right), and AA_0 (bottom) show common patterns for real-coded NSGA-II solutions on Problem 1.

per bound in the next hour, then continue with the same quantity for some more time and finally reduce close to the lower bound. This phenomenon can be explained as follows. A high amount of NaOH addition is required in the first phase of reaction process for a better initiation of polymerization (first three steps are responsible for chain initiation, as presented in appendix) and the amount of NaOH can be kept low in the later part of the process as mainly the growth of chain length (in appendix, last two steps are responsible for chain growth) occurs at that part of time and NaOH is produced as a by-product. The reason for NaOH to come down at the lower bound after the addition at the zeroth hour for some solutions is due to the fact that the initiation steps require NaOH as a reactant and also produce as a by-product. In case of M_n value less than 7.0×10^3 kg/kg mol, NaOH is found to be added in a systematic fashion. For M_n value greater than 7.0×10^3 kg/kg mol, NaOH, instead of decreasing at time step of the first hour after the first addition, goes up and rest of the trend remains same as it is stated earlier. In these cases, NaOH takes part not only in the initiation but also in growth of chain length by helping to form certain species of polymer (BE_n) which contributes significantly towards the high value of M_n.

(2) The trend found for epichlorohydrin is straightforward. It must be started at different levels depending on the required M_n value, but must be quickly increased close to the upper limit and must be continued at that amount till the end. The reason for small required value of epichlorohydrin initially is due to it having a less contribution in polymer chain initiation. However, epichlorohydrin should be supplied maximally in the later stages due to its major contribution in chain growth mechanisms. Also, more epichlorohydrin results in more BF_n, EF_n, and FF_n kind of polymer species in the ultimate polymer product. It is experienced by the authors that if the amount of epichlorohydrin is less (especially in the later part of the reaction process), one can expect more growth in AB_n and BB_n type of polymer species. So, based on the requirement of the process engineer, controlled species distribution can be achieved by different kind of intermediate additions.

(3) Bisphenol-A must be started in large amount and then must be reduced with time. This is because bisphenol-A takes part actively in polymerization initiation step and its requirement is reduced at the later part (in appendix, last two steps are responsible for chain growth). The addition is observed to prolong for longer time steps for higher values of M_n. This happens because a large M_n value is achieved by adding more amount of bisphenol-A in the system. It has been seen that the added bisphenol-A is consumed almost completely (i.e. not added more than the amount required) in most of the cases.

It is clear from these observations that different polymers (with different M_n and PDI values) must be produced optimally with a different addition pattern of reactants. Although this is intuitive, Fig. 6 shows a particular pattern of achieving them *optimally*.

To better understand the characteristics of solutions at different parts of the Pareto-optimal front, we divide the entire Pareto-optimal region into three groups and then discuss the

Table 1
Three representative solutions picked from the Pareto-optimal front obtained by real-coded NSGA-II in each of the three problems are shown

Source	PDI (kg/kg)	M_n (kg/kg mol)	Reaction time (h)
Benchmark	1.61	633.2	7.00
	Problem 1		
Group 1	1.59	926.5	7.00
Group 2	1.87	3186.1	7.00
Group 3	1.97	9507.8	7.00
	Problem 2		
Group 1	1.70	946.6	2.57
Group 2	1.90	3219.5	4.00
Group 3	1.99	9507.6	6.60
	Problem 3		
Group 1	1.61	943.71	3.80
Group 2	1.88	3218.02	5.17
Group 3	1.97	9508.45	6.98

properties of each group by choosing one representative solution from each group. This may be used to predict the addition patterns to be maintained when a process engineer picks up a solution from Pareto-optimal front and wants to manufacture the polymer of that specification. As the solutions on Pareto-optimal front span M_n from 0.4×10^3 kg/kg mol to almost 9.5×10^3 kg/kg mol, each region roughly spans 3.0×10^3 kg/kg mol in M_n-axis: 0.0–3.0×10^3 kg/kg mol M_n (Group 1), 3.0–6.0×10^3 kg/kg mol M_n (Group 2), and 6.0–9.0×10^3 kg/kg mol M_n (Group 3). The representative solution in each group are shown in Table 1 and the regions for each group is also marked in Fig. 5.The trend in the amount of addition of reactants for each group is shown in Fig. 7. Each group has a distinct pattern of adding the three reactants. For example, although in all cases the NaOH addition must be high in the middle of the reaction time span and must be drastically reduced soon thereafter, polymers with very small M_n values need to be produced with almost zero addition of NaOH at $t = 1$ h. Similarly, for producing polymers having very large M_n value, the comparatively small dosage of epichlorohydrin must be added initially $t=0$. Although such conclusions can be made by understanding the chemistry of the process, the above plots presents the trend quantitatively for a specific requirement of a polymer. We summarize these findings in the following:

Group 1: NaOH addition needs a delayed rise accompanied by a dip in first hour after starting from the low initial (lower bound) concentration; Epichlorohydrin addition needs a fast rise from low starting concentration; AA_0 addition needs a very quick fall from a somewhat high initial (near to upper bound) concentration.

Group 2: NaOH addition needs a delayed rise without any fall in between after starting from the low initial (lower bound) concentration; Epichlorohydrin additions needs a faster rise from relatively higher starting concentration; AA_0 addition needs a fall at the second hour starting from a high initial (upper bound) concentration.

Group 3: NaOH addition needs a sharp rise after starting from the low initial (lower bound) concentration; Epichlorohydrin addition needs a comparatively delayed rise from the low starting concentration; AA_0 addition needs a much

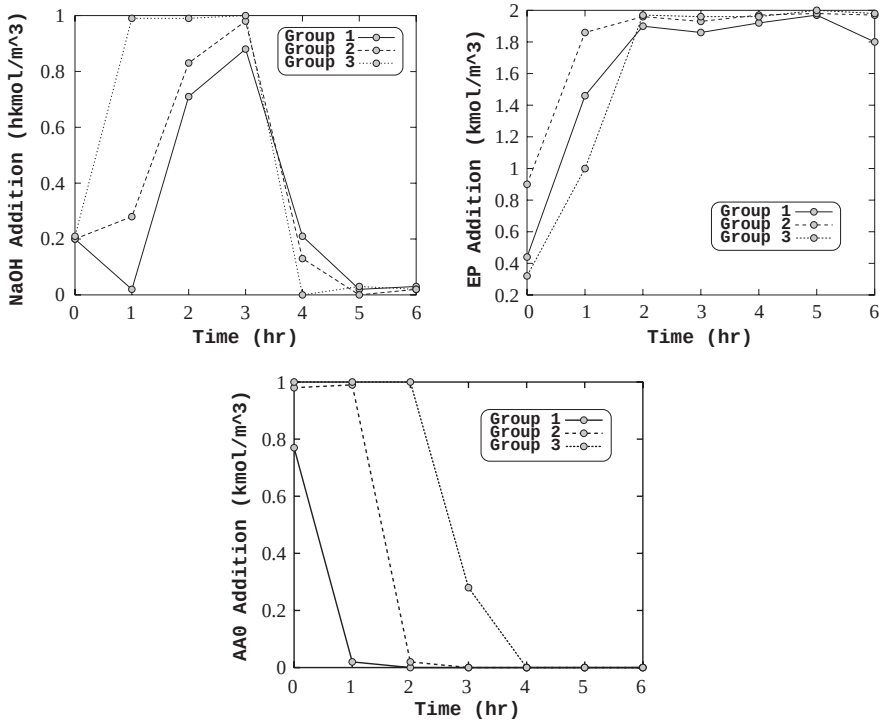

Fig. 7. Time-variant addition of NaOH (left), EP (middle), and AA_0 (right) are shown for three representative solutions from each group on the Pareto-optimal front obtained using the real-coded NSGA-II for Problem 1.

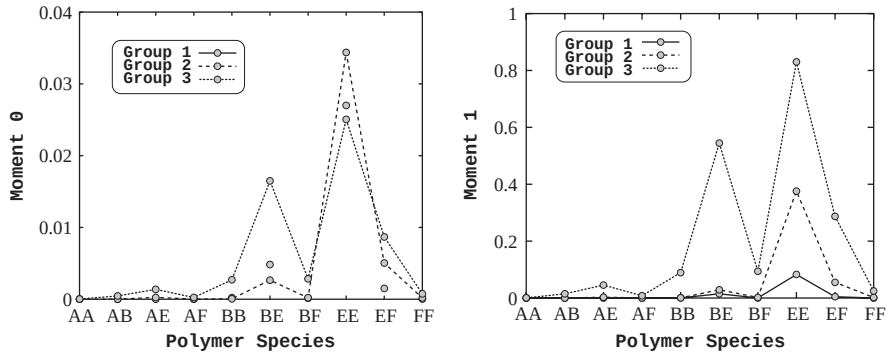

Fig. 8. Change in concentration (left) and first-order moment of different polymer species are shown for representative solutions from each group obtained using real-coded NSGA-II for the M_n and PDI optimization.

late (after the second hour) fall from the high initial (upper bound) concentration.

The information above conveys that there lies a relationship between the solutions in the Pareto-optimal front and the system under consideration. The relationship can be regarded as the 'blue-print' of the system. Given a set of objectives, certain properties emerge from the system, not arbitrarily, but following some basic properties of the system. This relationship between the property of the system and the solutions of the Pareto-optimal front would be of tremendous importance to process or production engineers. Such observation has also been observed in other engineering design problems such as gearbox design, truss-structure design, etc. (Deb, 2003) and in other chemical process optimization problems, such as in multi-objective optimization of various processes like grinding of lead zinc ore (Mitra and Gopinath, 2003), iron ore sintering process (Nath and Mitra, 2004). Various rules that are evolved while characterizing the Pareto-optimal front can be used as innovative and intelligent thumb rules for epoxy polymerization. Such intelligent rules, though appeared simple, cannot be predicted easily for a complex system like epoxy polymerization and requires a thorough study and can be proved to be beneficial for most of the industrial systems where operating rules are generally slowly developed on the basis of experience. Pareto characterization can help a process engineer to control the operation of an epoxy-polymerization reactor for maintaining different production schedules as well. Besides utilizing the mathematical optimality conditions outlined in standard texts (Deb, 2001; Miettinen, 1999), there exist no other methods to decipher such vital information about a complex problem.

As several polymer species are involved in this polymerization study, the next interest would be to investigate the distribution of various species at the end of polymerization. Fig. 8 (left plot) shows EE_n as a major product for polymers of lower dispersity and as dispersity increases, BE_n, another species, evolves as the nearest competitor. As the first-order moment is directly related to the growth in chain length, variation of different polymer species plotted against the first-order moment (the right plot in Fig. 8) shows the same trend. Polymer of higher M_n can be achieved by the growth of various other polymer species (BF_n, EF_n, BB_n), but as the number of species increases in the final distribution, the dispersity (PDI) also increases. The only way, therefore, to achieve higher M_n with a lower PDI is to have growth of any particular polymer species in course of polymerization. Here, for polymers having a higher PDI value, like one in Group 3, as more than one species start competing with the major species (EE_n), a higher M_n is achieved at the cost of a higher PDI value. For a process engineer, if a higher polydispersity value is desired, a polymer with a higher M_n value will be desired and otherwise not. Even, based on the type of the species, the process engineer can have choices among various options from the Pareto-optimal front solutions.

4.1.4. NSGA-II parametric study

The effect of varying GA parameters on the obtained Pareto-optimal front is studied next. If the population size is decreased from 250 to 100, the convergence rate is marginally faster (converging at iteration 27, instead of 34 iterations required with 250 population members), but the convergence speed is achieved at the cost of a poor spread of solutions on the front, especially towards the smaller PDI values. The effect of reducing the crossover probability (from 0.9 to 0.7) again leads to no significant change in converging and maintaining spread of solutions on the Pareto-optimal front. The effect of a change in the mutation probability (from 0.1 to 0.01) indicates no significant change as well. However, when the distribution index of the SBX operator is changed gradually from 0.01 to 100, a slightly inferior spread of Pareto-optimal solutions is obtained. When the distribution index for polynomial mutation operator is changed gradually from 0.01 to 100, a better spread of Pareto-optimal solutions is observed. In all cases, the performance is compared by keeping the same number of overall solution evaluations. Since the chosen NSGA-II parameter values (as described in Problem 1) produce reasonably good convergence and maintenance of spread of solutions, we continue the rest of the simulations with these values.

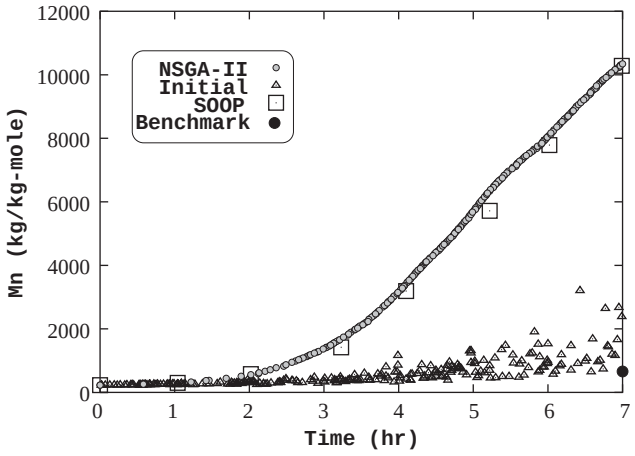

Fig. 9. Obtained NSGA-II solutions for the M_n and reaction time optimization are compared with single-objective optimization (SOOP) solutions. Initial solutions of NSGA-II and the benchmark solution are also shown.

4.2. Discussion on Problem 2

Next, we turn our attention to the optimization of M_n and the reaction time. The reaction time is also treated as an additional decision variable. The same upper and lower bounds for reactants are kept for this case also, only addition being the reaction time which is varied as follows: $0 \leqslant t_{\text{sim}} \leqslant 7$ h. After the multi-objective optimization with NSGA-II, Pareto-optimal solutions (marked as 'NSGA-II') are plotted in Fig. 9. To show the progress made by NSGA-II over iterations, the randomly created initial solutions are also shown as "Initial" in the figure. Once again, the random solutions within the chosen variable bounds are far from being close to the true Pareto-optimal front and NSGA-II is able to find a wide range of solutions starting with these random solutions. The generic observation is that a smaller reaction time produces polymers having a smaller M_n value. Once again, the M_n-time optimality front seems to be non-convex.

Like before, the ε-constraint method is used to constrain the reaction time values and M_n is maximized. A number of solutions (marked as 'SOOP') obtained with this repeatedly applied single-objective formulation are also shown in Fig. 9. Both the NSGA-II and the single-objective GA solutions agree at most cases (in other cases, NSGA-II solutions are better), thereby establishing confidence in the optimality of the obtained solutions.

The NSGA-II solutions are much better than the benchmark solution, as shown in Fig. 9. Among many solutions from the Pareto-optimal front obtained using the real-coded NSGA-II, one solution is chosen for demonstrating how the same quality polymer (having the same order of magnitude of M_n and PDI as compared to the benchmark solution) can be obtained in a much less processing time. A polymer having M_n value of 616 kg/kg mol and PDI value of 1.57 is compared with the benchmark solutions (M_n of 633.2 kg/kg mol and PDI of 1.61 obtained with 7 h of reaction time). The obtained NSGA-II solution requires only 2.13 h of reaction time, thereby requiring less than one-third time of completion from the benchmark solution. This is equivalent to a 300% improvement in the productivity. In general, in case of Problem 2, it has been observed that by manipulating several reactant addition amounts, a similar quality polymer (as compared to that obtained in Problem 1) can be obtained in a much less processing time. But since the PDI minimization is not performed in Problem 2, for similar M_n values in both cases, PDI values for the M_n-time Pareto-optimal solutions (Problem 2) are higher as compared to the same for Problem 1. This calls for an optimization of all three objectives for a better solution, a matter which we deal in Section 4.3.

4.2.1. Analyzing the solutions of Problem 2

In Problem 2, each of the solutions on the Pareto-optimal front carries information of 22 decision variables. A similar investigation, as done in Problem 1, is intended to carry out next to identify whether these solutions on the time Pareto-optimal front have some commonality among themselves. As the reaction time is a variable here, it is not easy to perform a trend analysis similar to that used in Problem 1. Fig. 10 compares the characteristics of equivalent solutions (having similar M_n values) taken from the Pareto-optimal front of Problems 1 and 2. Table 1 showed these chosen solutions from the three groups in both fronts. It can be stated that in case of Problem 2, though the patterns for addition of epichlorohydrin and bisphenol-A are almost similar to those in case of Problem 1, the reduction in time is mainly achieved by adding more NaOH into the system right from the start of the reaction process. That is, for preparing a polymer having a similar value of M_n as that obtained in Problem 1, the reaction time is found to be reduced drastically in Problem 2 as compared to the fixed reaction time of 7 h (for Problem 1) by increasing the initial addition of NaOH, but at a cost of a slightly higher PDI value. As more and more NaOH, EP and AA_0 are added to the system, secondary species like BE_n, EE_n, BF_n, EF_n get generated (as compared to the primary species BB_n, AB_n) in the system contributing significantly in increasing the M_n value and by parallely increasing the PDI value. This is due to the fact that an increase in number of species increases the dispersity value.

Fig. 10 clearly shows that although similar quality polymers are produced by both optimizations, their operating principles are quite different. The top row shows the addition trend of NaOH, EP and AA_0 for two equivalent solutions from the low M_n group (Group 1). The middle row shows the same for the intermediate M_n group (Group 2) and the bottom row shows the same for the high M_n group (Group 3). The dashed pattern is for the 7 h long solution obtained in Problem 1, whereas the solid pattern is obtained in Problem 2. For the latter case, the end of reaction time is shown by a vertical downward arrow.

The general trend captured in the NaOH addition is that NaOH must be added at a high quantity to start with, then

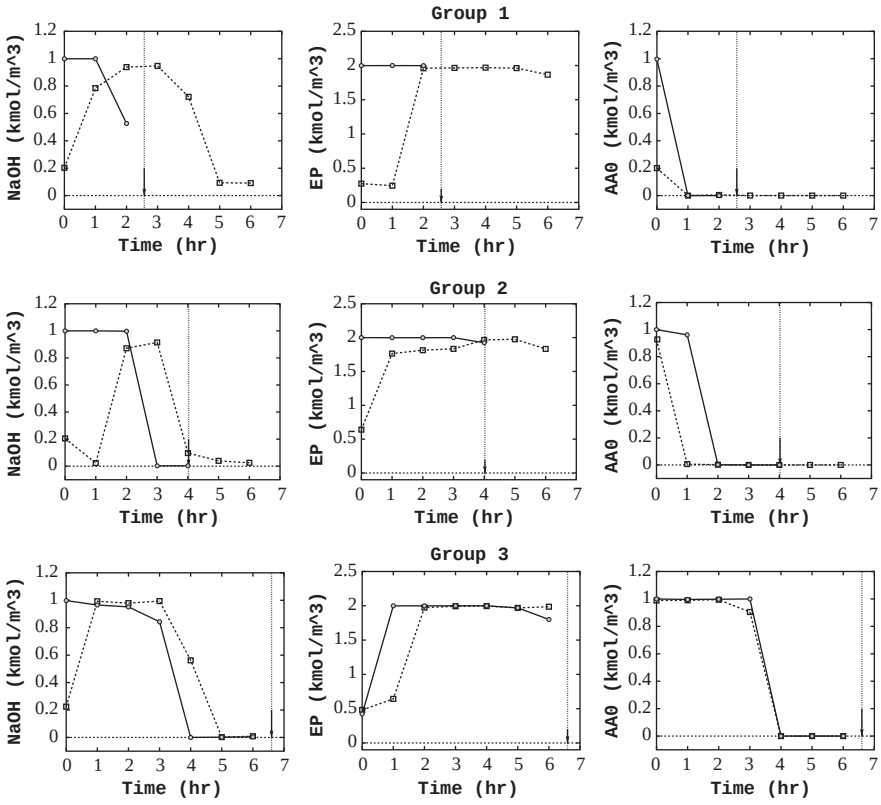

Fig. 10. Effect of reaction time minimization on three equivalent optimal solutions from Problems 1 and 2. Each row shows the comparison on a particular group. The dashed line is taken from Problem 1 and solid line is taken from Problem 2.

must continue with a similar amount for some time and then must be reduced. Here, NaOH is realized to take part not only in the initiation process, but also in the growth of the chain length. Epichlorohydrin (EP), on the other hand, is found to be needed more (as compared to Problem 1) in the beginning for low and medium M_n requirement, but for high M_n values, EP addition needs to be slowed down in the beginning. Trends for bisphenol-A (AA_0) remain almost the same as in Problem 1 (that is, adding more in the beginning and using the same for polymerization for the rest of the time). Barring the details, it can be concluded that although all three reactants are required to be added more in the beginning (in comparison to a 7 h long polymerization process) to achieve a similar polymer in a smaller time, the addition patterns of reactants, requiring the formation of the desired polymer are similar.

Next, the species distribution for all three groups mentioned in Table 1 for Problem 2 is plotted in terms of moment zero (left plot in Fig. 11) and the first-order moment (right plot in Fig. 11) carrying information on concentration of species and growth of chain length, respectively. From the left plot in Fig. 11, it can be seen that the species BB_n (AB_n being its close competitor) is a primary species and there is a clear shift towards BE_n, BF_n, EE_n, and EF_n for the cases with higher time and M_n. In fact, with more addition of NaOH, epichlorohydrin and higher bisphenol-A affect the process for producing more BE_n, BF_n, EE_n, and EF_n type of polymer species. Similarly first moments for all the cases have also indicated a large growth in chain length for BE_n, BF_n, EE_n, and EF_n type of species for a longer time and a higher M_n value (right plot in Fig. 11).

4.3. Discussion on Problem 3

The Pareto-optimal solutions for three objective optimization problem (henceforth called as 'three-dimensional Pareto-optimal front') are plotted in Fig. 12.

When the previously obtained two fronts (from Problems 1 and 2) are drawn on this plot, they are interestingly found to be the limiting fronts lying on the two edges of the three-dimensional front. First, we deduce the following conclusions from the three-dimensional front:

(1) The three-dimensional Pareto-optimal front is a non-convex front.
(2) For low values of M_n, polymers can be prepared in much less than 7 h. Since the reaction time is also minimized in Problem 3, there exists almost no solution requiring as large as 7 h to produce a polymer having a low M_n.
(3) For high values of M_n, more reaction time is needed. As in the polymerization process, the repeat units get

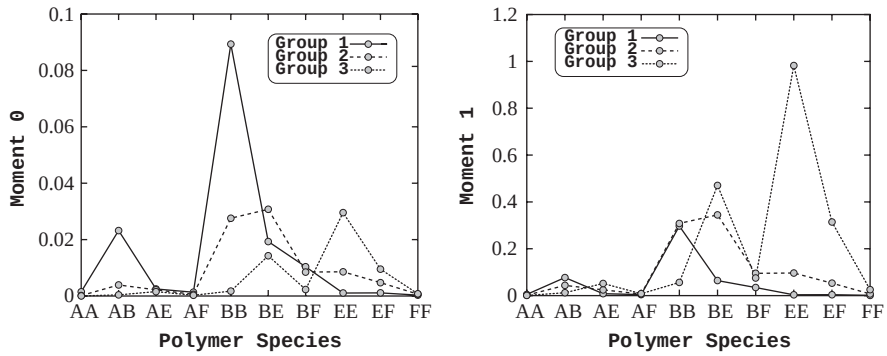

Fig. 11. Change in concentration (left) and first-order moment of different polymer species are shown for representative solutions from each group obtained using real-coded NSGA-II for the M_n and reaction time optimization for Problem 2.

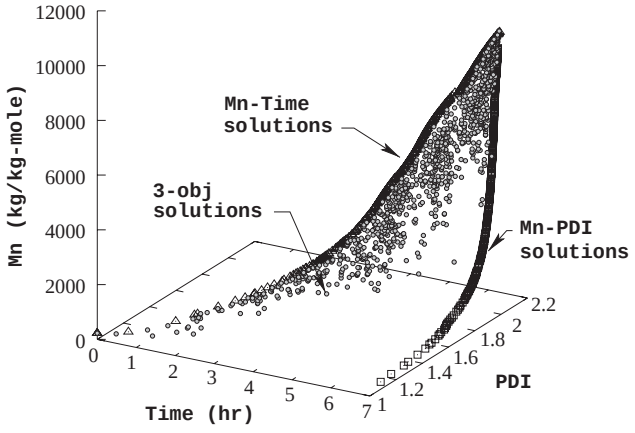

Fig. 12. NSGA-II solutions obtained from the three-objective optimization are shown. The fronts obtained in the previous two problems are found to lie on two edges of the obtained three-dimensional front.

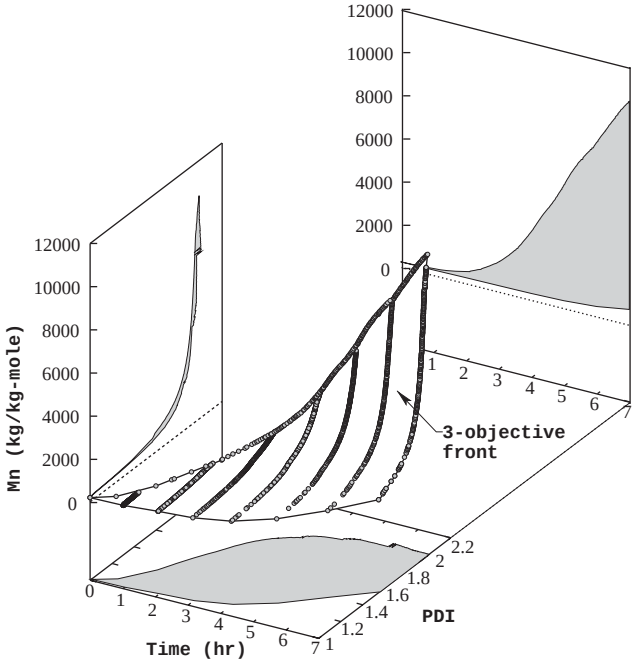

Fig. 13. Several optimizations of Problem 1 with different t_{sim} values help find the third boundary of true three-dimensional Pareto-optimal front.

added with the monomer to form a longer chain length, a polymer having a high value of M_n requires more time to form than a polymer having a low value of M_n. But for a desired M_n and PDI combination, one can find a solution requiring smaller than 7 h to do the job, but the occurrence of such a quick operation gets reduced with the requirement of higher and higher M_n values.

(4) Finally, for the maximum M_n requirement, there exists only one solution (with $M_n = 10,402.12$ kg/kg mol), requiring 7 h (the maximum allowed) of reaction time, but also producing the largest PDI value (1.985). Such is the trade-off often observed in multi-objective optimization problems and Fig. 12 shows many such trade-off solutions producing different values of M_n and PDI and requiring different amount of reaction time.

(5) Another interesting aspect is that for any fixed reaction time, the M_n-time optimization (Problem 2) solutions produced the maximum M_n value and there exists no other solution producing a better (smaller) PDI value and an identical M_n value. But, the three-dimensional Pareto-optimal front provides more information about the trade-off than both two-objective Pareto-optimal fronts, discussed earlier.

On the three-dimensional Pareto-optimal front, there seems to be a larger concentration of solutions towards the M_n-time front (in other words, there are more solutions requiring a smaller processing time). To understand this trend better, we repeat Problem 1 for different reaction times. We force the reaction time to end at $t_{\text{sim}} = 1$ h, 2 h, and so on, and collect all the obtained Pareto-optimal solutions. Thereafter, we perform a non-domination check considering all three objectives (maximization of M_n, minimization of PDI, and minimization of t_{sim}) and the resulting solutions are plotted in Fig. 13. An interesting aspect is revealed. For identical PDI values, there exists a smaller reaction

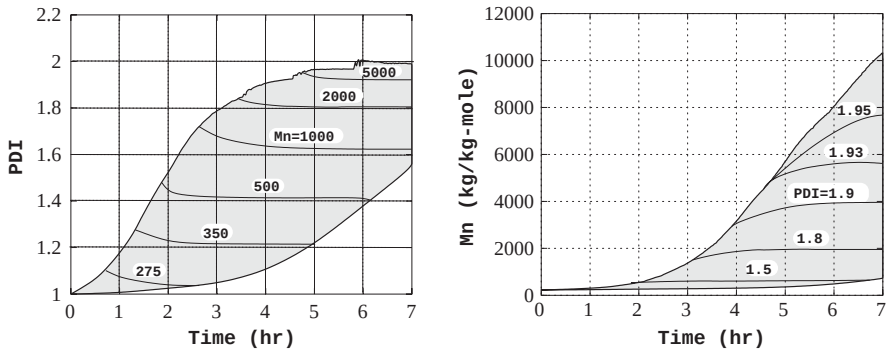

Fig. 14. PDI and reaction time interaction (left) and M_n and reaction time interaction (right) reveal interesting properties about the *optimal operating conditions* of the polymerization problem. In the left figure, M_n is shown in kg/kg mol.

time solution outperforming a larger time solution. This feature of the problem produces a *third* boundary on this three-dimensional Pareto-optimal front, thereby showing the complete bounded trade-off surface of interactions. The figure also shows the projection of the three-dimensional trade-off surface on the three two-objective planes. It is clear that although there are some rooms for trade-offs among M_n-time and PDI-time combinations, in terms of M_n-PDI combinations, there is almost a straightforward trade-off. This fact also indicates that the consideration of minimization of the reaction time is important in this problem to reveal interesting time-saving trade-off solutions.

To understand the three-objective interactions further, we consider the PDI-time and M_n-time projections (as shown shaded in Fig. 13) and plot them again in Fig. 14 in the left and right plots, respectively. On the PDI-time plot, we show contours of fixed M_n values. For each contour line, the trade-off between PDI and reaction time is clear. However, what is more interesting is that the trade-off becomes marginal away from the M_n-time Pareto-optimal front (the upper boundary). To achieve a small advantage in the PDI value, a large reaction time is necessary. Since the slope of the three-objective Pareto-optimal front is quite small at these regions, the NSGA-II has found very few solutions away from the M_n-time boundary in Fig. 12. It can then be concluded that for a fixed M_n requirement, it is better to consider the trade-off solutions close to the M_n-time Pareto-optimal boundary. Another aspect is the rate at which the 'region of optimality' reduces for an increasing M_n value. For example, if a polymer with M_n greater than 5000 kg/kg mol is desired, there does not exist too many options in terms of the reaction time. The right plot in Fig. 14 shows contour lines for fixed values of PDI on the three-objective Pareto-optimal front. Once again the trade-off between M_n and reaction time is clear from the plot. Although a similar conclusion (about choosing solutions close to the M_n-time optimal boundary) can be made for smaller PDI values, for large PDI values (such as PDI = 1.95) the trade-off between M_n and reaction time is quite substantial. These two plots can be chosen to determine a suitable operating condition for the epoxy-polymerization problem.

Once again, like Problems 1 and 2, representative solutions are chosen for analysis from the three groups of M_n (see Table 1). It can be easily observed that in case of Problem 3, similar M_n (943.71 kg/kg mol as compared to 946.6 kg/kg mol of Problem 2) can be achieved with a smaller PDI (1.61 as compared to 1.70 of Problem 2), but at the cost of a little more reaction time (3.80 h as compared to 2.57 h). This was one difficulty in Problem 2 stated earlier: similar M_n is achieved at the cost of more PDI, but with the smallest possible reaction time. This trade-off between PDI and time can be very effectively used by a process engineer for different kinds of operations, i.e. the engineer can choose a solution from the results of Problem 3 if the product quality is extremely important for a client (of course, at the cost of productivity) or choose a solution from the results of Problem 2 if the product quality requirement is not so stringent, but the productivity is of utmost importance. For example, one solution of Problem 3 recommends $M_n = 630$ kg/kg mol, PDI = 1.54 and reaction time equal to 2.27 h, but for the benchmark case, they are as follows: $M_n = 631$, PDI = 1.61 and reaction time equal to 7 h. So, a much better quality polymer (with reduced polydispersity) can be produced in less than one-third of the actual reaction time (recommending more than 300% productivity improvement). Although the Problem 2 finds two similar polymers (with $M_n = 616$ and 666 kg/kg mol) in slightly less reaction times (2.13 and 2.21 h, respectively), the PDI values (1.57 and 1.60, respectively) are slightly inferior. This shows the effectiveness of using all three objectives in a study, where all of them are important in the decision-making process.

The extreme solutions are extracted from the above studies and are presented in Table 2. For a fixed reaction time, the trade-off between M_n and PDI is clear from the table. Interestingly, Fig. 13 also indicates that there exist polymers with a continuous variation of M_n and PDI between the two extreme cases for each reaction time shown in the table.

The three-objective optimization study also leads to the investigation of species distribution for the groups presented in Table 1 (Problem 3). Both the zeroth and the first-order moments are shown for these groups in left and right plots in Fig. 15, respectively. It is clear from the figures that in

Table 2
Extreme polymers extracted from the three-objective Pareto-optimal front (Fig. 13) for different reaction times of the epoxy-polymerization process

Reaction	Maximum M_n		Minimum PDI	
time (h)	M_n (kg/kg mol)	PDI	M_n (kg/kg mol)	PDI
1	294.524	1.147	238.519	1.005
2	561.872	1.522	236.751	1.008
3	1379.881	1.788	268.711	1.034
4	3162.372	1.906	282.337	1.069
5	5333.817	1.934	289.212	1.075
6	7949.621	1.966	279.515	1.096
7	10402.122	1.985	271.734	1.083

Problem 3, there is no development of new species in the course of the polymerization (as also observed in Problem 2) and distribution of species is much organized in these two cases. Here, BE_n and EE_n are the primary species when M_n requirement is low. With a larger requirement of M_n, secondary species, like BB_n, BF_n, and EF_n, get generated, a phenomenon which was observed with solutions from Problem 1 as well.

5. Conclusions and extensions

A well-validated model consisting of a large number of moment-based ordinary differential equations has been utilized for the multi-objective optimization of epoxy-polymerization process using an evolutionary algorithm (NSGA-II). The aim of the study has been to extract the discrete addition patterns of the reactants for optimizing various objectives simultaneously (e.g. Problem 1: Maximization of M_n with minimization of PDI, Problem 2: Maximization of M_n with minimization of reaction time and Problem 3: Maximization of M_n, minimization of PDI, and minimization of reaction time). The salient features which resulted from this work are:

(1) Solutions to Problem 1 have led to better M_n (higher) and PDI (lower) values as compared to the available benchmark data on the problem. Solutions to Problems 2 and 3 have provided optimal operating conditions of producing polymers with a similar M_n, but with a smaller PDI value in as much as one-third of the reaction time (as compared to benchmark solution).
(2) Importantly, the multi-objective optimization of the epoxy-polymerization process has led to the discovery of certain operating principles (addition time-pattern of three reactants (NaOH, Epichlorohydrin, and Bisphenol-A)) for all high-performance solutions. The trade-off between the objectives have been clearly characterized by showing and contrasting a representative additive pattern of all three reactants. Such a piece of information brings out the 'blue-print' of the optimal operating conditions of a chemical process and is often important from the point of view of a process or production engineer.
(3) The distribution of various species for all three problems has been studied to show how a change in reactant addition pattern has changed different species distribution during the course of polymerization. This study has also showed the change in the distribution of various species for different degrees of polymerization, which has provided further insight into the underlying process.
(4) Semi-batch mode of operations for epoxy processes has been found to be much superior to the benchmark, one-time addition processes (batch mode).
(5) The study of multi-objective optimization on all three objectives has demonstrated a systematic procedure of identifying the overall trade-off relationship among the objectives. Since the NSGA-II procedure is capable of finding multiple Pareto-optimal solutions with a good spread in them, it has been possible to perform such a study. Once such a trade-off relationship is identified and a mapping of every solution from the trade-off surface to the corresponding decision variables is established, such information can be used an 'operating chart' for performing an optimal operation. For a desired requirement in any combination of objectives, a suitable operating solution can be found from such a chart.

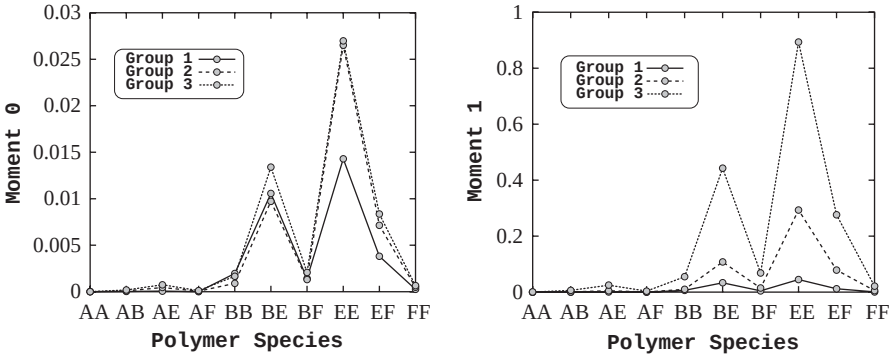

Fig. 15. Change in concentration (left) and first-order moment of different polymer species are shown for representative solutions from each group obtained using real-coded NSGA-II for the M_n, PDI, and reaction time optimization.

(6) All three problems considered here have displayed a non-convex Pareto-optimal front. NSGA-II has been able to find solutions on or near the true Pareto-optimal front of the problems. This has been validated by solving the multi-objective problems using a single-objective preference based optimization method (ε-constraint method). The advantage of using the NSGA-II is that it has found multiple (as many as 250) Pareto-optimal solutions in a single simulation run.

The two-objective optimization problems took about 3 h of computational time on a Pentium IV 1.5 GHz processor and the three-objective optimization problem took about 13 h on the same machine. However, since such a study is expected to be performed off-line and once for a particular process for the purpose of understanding the process better, such tasks providing useful information discussed above are worth the effort.

This study used some primary oligomer concentration profiles available as experimental data. With the availability of more such experimental data, the underlying mathematical model can be improved further. In fact, using the recommendations of this optimization study, experiments now can be performed and effectiveness of the current recommendations can be validated as well. Specific growth of a particular polymer species out of several considered here can also be performed depending on the requirements of the industry. Nevertheless, this extensive study has clearly demonstrated the use of a multi-objective optimization procedure in understanding a complex process, such as the epoxy-polymerization process, and outlined a systematic optimization procedure for arriving at the optimal operating chart with a clear trade-off information about salient objectives of the process—a matter which would ultimately have a tremendous practical importance.

Notation

AA_0	bisphenol-A (monomer)
AB_m	molecular species (polymer)
B	sodium phenoxide end group
d_i	crowding distance of ith population member
E	glycidyl ether group
EP	epichlorohydrin
F	chlorohydrin end group
F_i	ith fitness function
I_{ij}	jth objective function for the ith problem
I_i	objective function vector of the ith problem
K_i	reaction rate constant
M_n	number average molecular weight (kg/kg mol)
M_w	weight average molecular weight (kg/kg mol)
NaOH	sodium hydroxide
n	number of u_i values used in NSGA-II
N_{Gen}	iteration number
$N_{\text{Gen,max}}$	maximum number of iterations
N_{Pop}	number of solutions in the NSGA-II population
P_N	parent population at Nth iteration
p_m	mutation probability
p_c	crossover probability
PDI	poly-dispersity index (M_w/M_n)
Q_N	offspring population at Nth iteration
R_N	combined population at Nth iteration
t_{sim}	reaction time (h)
t_j	discrete time instants for adding reactants (h)
U	vector of control variables,$U_1(t_j)$,$U_2(t_j)$, $U_3(t_j)$
$U^{(i)}_{\text{pop,j}}$	value of control variable at the end of kth time interval for ith solution
$U^{\max}_{\text{pop,j}}$,$U^{\min}_{\text{pop,j}}$	upper and lower bounds on control variable at the end of kth time interval
x	vector of state variables,x_i
δ_{m0}	a factor (0 for molecular weight determination without epichlorohydrin and 1 with epichlorohydrin)
$[\bullet]$	concentrations

Acknowledgements

Authors acknowledge the support of TRDDC as well as TCS management in the course of this work. K. Deb acknowledges the Bessel Research award from Alexander von Humboldt Foundation Germany.

Reaction scheme for epoxy polymerization

Here, we present five reaction schemes of the epoxy-polymerization process. The details can be found in Majumdar et al. (2004) and in Raha and Gupta (1998).

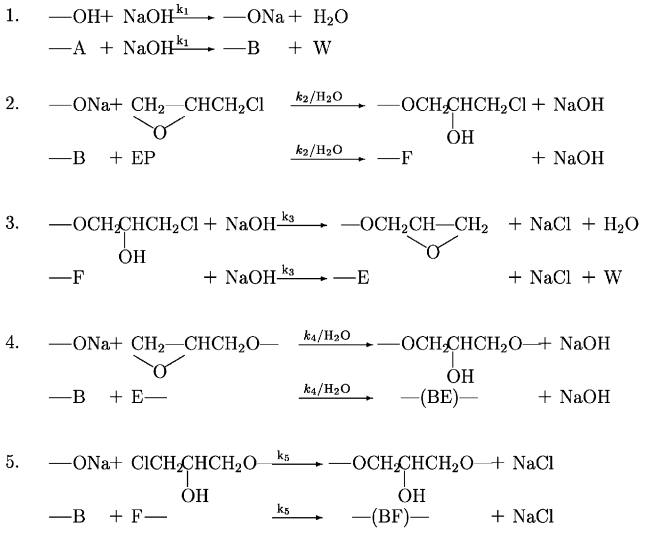

The end groups present in the reaction mass are as follows:

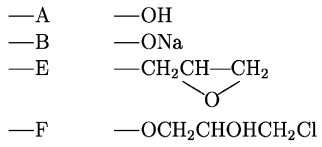

References

Batzer, H., Zahir, S.S., 1977. Studies in the molecular weight distribution of epoxide resins. IV. Molecular weight distribution of epoxide resins made from bisphenol-A and epichlorohydrin. Journal of Applied Polymer Science 21, 1843–1857.

Bhaskar, V., Gupta, S.K., Ray, A.K., 2000. Applications of multi-objective optimization in chemical engineering. Reviews in Chemical Engineering 16 (1), 1–54.

Butala, D., Choi, K.Y., Fan, M.K.H., 1988. Multiobjective dynamic optimization of a semibatch free-radical copolymerization process with interactive CAD tools. Computational Chemistry and Engineering 12, 1115.

Chakravarthy, S.S.S., Saraf, D.N., Gupta, S.K., 1997. Use of genetic algorithms in the optimization of free radical polymerizations exhibiting the Trommsdorff effect. Journal of Applied Polymer Science 63, 529.

Chankong, V., Haimes, Y.Y., 1983. Multiobjective Decision Making—Theory and Methodology. Elsevier, New York.

Choi, K.Y., Butala, D.N., 1991. An experimental-study of multi-objective dynamic optimization of a semibatch copolymerization process. Polymer Engineering Science 31, 353–364.

Deb, K., 2000. An efficient constraint handling method for genetic algorithms. Computer Methods in Applied Mechanics and Engineering 186, 311–338.

Deb, K., 2001. Multi-objective Optimization Using Evolutionary Algorithms. Wiley, Chichester, UK.

Deb, K., 2003. Unveiling innovative design principles by means of multiple conflicting objectives. Engineering Optimization 35 (5), 445–470.

Deb, K., Agrawal, R.B., 1995. Simulated binary crossover for continuous search space. Complex Systems 9 (2), 115–148.

Deb, K., Pratap, A., Agarwal, S., Meyarivan, T., 2002. A fast and elitist multi-objective genetic algorithms. IEEE Transactions on Evolutionary Computation 6 (2), 182.

Fan, L.T., Landis, C.S., Patel, S.A., 1984. In: Doraiswamy, L.K., Mashelkar, R.A. (Eds.), Frontiers in Chemical Reaction Engineering. Wiley Eastern, New Delhi, p. 609.

Farber, J.N., 1986. Steady state multiobjective optimization of continuous copolymerization reactors. Polymer Engineering Science 26, 499–507.

Farber, J.N., 1989. In: Cheremisinoff, N.P. (Ed.), Handbook of Polymer Science and Technology, vol. 1. Dekker, New York, p. 429.

Garg, S., Gupta, S.K., 1999. Multiobjective optimization of a free radical bulk polymerization reactor using genetic algorithm. Macromolecular Theory and Simulations 8, 46–53.

Garg, S., Gupta, S.K., Saraf, D.N., 1999. On-line optimization of free radical bulk polymerization reactors in the presence of equipment failure. Journal of Applied Polymer Science 71, 2101–2120.

Goldberg, D.E., 1989. Genetic Algorithms in Search, Optimization and Machine Learning. Addition-Wesley, Reading, MA.

Gupta, R.R., Gupta, S.K., 1999. Multi-objective optimization of an industrial Nylon-6 semibatch reactor system using genetic algorithm. Journal of Applied Polymer Science 73, 729–739.

Kumar, A., Gupta, S.K., 1987. Reaction Engineering of Step Growth Polymerization. Plenum, New York.

Majumdar, S., Mitra, K., Raha, S., 2004. Analysis of semibatch operation in epoxy polymerization, in press.

McAdams, L.V., Gannon, J.A., 1986. Encyclopedia of Polymer Science and Engineering, vol. 6, second ed. Wiley, New York, 322p.

Miettinen, K., 1999. Nonlinear Multiobjective Optimization. Kluwer, Boston.

Mitra, K., Gopinath, R., 2003. Multiobjective optimization of an industrial grinding operation using elitist nondominated sorting genetic algorithm. Journal of Chemical Engineering Science 59, 385–396.

Mitra, K., Deb, K., Gupta, S.K., 1998. Multi-objective dynamic optimization of an industrial nylon 6 semibatch reactor using genetic algorithm. Journal of Applied Polymer Science 69, 69.

Nath, N.K., Mitra, K., 2004. Mathematical modeling and optimization of two-layer sintering process for sinter quality and fuel efficiency by genetic algorithms. Materials and Manufacturing Processes, in press.

Raha, S., Gupta, S.K., 1998. A general kinetic model for epoxy polymerization. Journal of Applied Polymer Science 70, 1859.

Raha, S., Majumdar, S., Mitra, K., 2004. Effect of caustic addition in epoxy polymerization process: a single and multi-objective evolutionary approach, Macromolecular Theory and Simulation. Macromolecular Theory Simulation 13, 152–161.

Ray, W.H., 1972. On the mathematical modeling of polymerization reactors. Journal of Macromolecular Science, Reviews in Macromolcular Chemistry C8 (1),

Sareen, R., Gupta, S.K., 1995. Multiobjective optimization of an industrial semibatch nylon 6 reactor. Journal of Applied Polymer Science 58, 2357–2371.

Srinivas, N., Deb, K., 1995. Multiobjective function optimization using nondominated sorting genetic algorithms. Evolutionary Computation 2 (3),

Tsoukas, A., Tirrell, M.V., Stephanopoulos, G., 1982. Multi-objective dynamic optimization of semibatch copolymerization reactors. Chemical Engineering Science 37, 1785–1795.

Wajge, R.M., Gupta, S.K., 1994. Multiobjective dynamic optimization for a nonvaporizing nylon-6 batch reactor. Polymer Engineering Science 34, 1161–1172.